Long-range electron-electron interactions in graphene make its electrodynamics nonlocal

B. Rosenstein,[1,2] H. C. Kao,[3] and M. Lewkowicz[2]
[1]*Electrophysics Department, National Chiao Tung University, Hsinchu 30050, Taiwan, Republic of China*
[2]*Physics Department, Ariel University, Ariel 40700, Israel*
[3]*Physics Department, National Taiwan Normal University, Taipei 11677, Taiwan, Republic of China*
(Received 6 May 2014; revised manuscript received 1 July 2014; published 28 July 2014)

Graphene, a one-layer-thick hexagonal array of carbon atoms, when undoped, exhibits a curious mixture of properties pertinent to either metals or insulators. On the one hand, despite near absence of both charge carriers and impurities, it has a finite conductivity like a metal. On the other hand, the Coulomb interaction between electrons is unscreened like in a dielectric and hence is long range. The chemical potential is pinned right between the conical valence and conduction bands causing quasiparticles to move like massless relativistic particles. We demonstrate at small coupling that the electrodynamics of graphene exhibits nonlocality on a macroscopic level due to the combination of the long-range interactions and the linear dispersion relation. The frequency and wave vector **k**-dependent conductivity tensor, in addition to a local pseudo-Ohmic part $\sigma_T\delta_{ij}$, possesses a nonlocal contribution $\sigma_{\rm nl}k_ik_j/k^2$. While the coefficient of the local part is $\sigma_T \approx e^2/4\hbar$, the coefficient of the nonlocal part is proportional to the Coulomb interaction strength α, $\sigma_{\rm nl} = \sigma_T\alpha$. This leads to several remarkable effects in transport and optical response. In particular, the resistance of the graphene flake depends on the location and the geometry of the source, drain, and probes. A voltage perpendicular to the current appears in a time-reversal symmetric situation and the polarization of reflected and transmitted light is modified, without either the magnetic field (like in the Faraday effect) or anisotropy.

DOI: 10.1103/PhysRevB.90.045137 PACS number(s): 72.80.Vp, 73.25.+i, 73.22.Pr, 78.67.Wj

I. INTRODUCTION

One of the basic assumptions of the electrodynamics in electrically active media is that the effect of electric fields can be described macroscopically by constitutive relations connecting the "induced" charges and currents to the electric field. For Fourier components for frequency ω and wave vector k, these relations (within linear response and neglecting magnetism) generally read

$$4\pi\rho^{\rm ind}(\omega,k) = i(1-\varepsilon(\omega,k))k_iE_i(\omega,k);$$
$$J_i(\omega,k) = \sigma_{ij}(\omega,k)E_j(\omega,k). \quad (1)$$

Usually the electrodynamic response of a medium is local, so that the long-wavelength limit exists. The dielectric constant then can be approximated by $\varepsilon(\omega,k=0)\equiv\varepsilon(\omega)$, while the conductivity tensor in an isotropic time-reversal invariant material takes a simple form:

$$\sigma_{ij}(\omega,k) = \delta_{ij}\sigma_T(\omega) + O(k^2). \quad (2)$$

The microscopic origin of the locality depends on the nature of the long-wave excitations and presence of long-range interaction between them. In an insulator (or semiconductor at low temperatures), the electronic excitations are gapped, so the locality is simply a result of absence of gapless charged excitations. In the free-electron gas model of a metal, i.e., neglecting both disorder and electron-electron interactions, there is no energy gap, so that the locality is not ensured. The conductivity tensor can be decomposed into a transversal and a longitudinal part (assuming time-reversal invariance and isotropy):

$$\sigma_{ij}(\omega,k) = \left(\delta_{ij} - \frac{k_ik_j}{k^2}\right)\sigma_T(\omega,k) + \frac{k_ik_j}{k^2}\sigma_L(\omega,k)$$
$$= \delta_{ij}\sigma_T(\omega,k) + \frac{k_ik_j}{k^2}\sigma_{\rm nl}(\omega,k). \quad (3)$$

Yet, the direct calculation [1] shows that the difference $\sigma_{\rm nl}(\omega,k) = \sigma_L(\omega,k) - \sigma_T(\omega,k) = O(k^2)$, thus leading to Eq. (2) with the corrections being analytic when $k\to 0$, namely, local.

Impurities define a scale, the mean free path, that effectively makes the excitations "massive" in terms of their dispersion relation. Composite excitations like diffusons can in principle have zero modes, but they are "soft" enough to cause the so-called "infrared divergencies" that could make the long-wave limit singular. In a very clean electron gas, the nonlocality can, in principle, arise due to long-range Coulomb interactions. However, the long-range interactions exist only in insulators. In a metallic state, the nonlocality is prevented by the screening of the Coulomb force that becomes effectively short-range and unable to cause infrared divergencies.

All the above three reasons leading to locality, namely, direct energy gap, significant disorder, and screening of the Coulomb interactions, are inapplicable to graphene. The novelty of the physics of the undoped graphene is mostly due to its spectrum of the elementary excitations. The dispersion relation at small momentum is linear [2], $\varepsilon_{\mathbf{k}} = vk$ (with $v\approx c/300$ being the Fermi velocity) and resembles massless relativistic fermions despite the fact that effects of static interactions make the dynamics nonrelativistic. The low-energy excitations belong to two conical bands joined in one of two "Dirac points." The chemical potential is pinned exactly at these points. Therefore there is no finite energy gap to ensure locality as in insulators.

The disorder also cannot ensure the locality in best graphene samples. In fact, graphene is one of the purest electronic systems. The scattering of charge carriers in suspended graphene samples of submicrometer length is so negligible that the transport is ballistic [3,4]. Consequently, the elementary excitations are still "massless" at long wavelengths. The third reason, interactions, also does not apply. If the interaction

between the quasiparticles was short range, one would still get a local electric response, but it turns out that the undoped graphene is apparently unable to screen the Coulomb interactions. So that there is no good reason to exclude the possibility that the long-wave electric response of graphene in the presence of strong interactions is nonlocal.

In this paper, we show that this is indeed the case and point out several consequences of that fact. The nonlocal part is proportional to the electron-electron interaction strength (when perturbation theory in interactions is valid):

$$\sigma_{\rm nl}(\omega,k) = -\frac{e^2}{4\hbar}\alpha + O(k^2), \tag{4}$$

where the coupling is $\alpha = e^2/\epsilon\hbar v$ with ϵ being the dielectric constant of the substrate, if present. This is the main result of the paper. The nonlocality of graphene, or more generally 2D (or even 3D [5]) electronic systems with similar band structure possessing a pointlike Fermi "surface"—nowadays termed Weyl semimetals—constitutes therefore the first example of the nonlocal electrically active medium.

The paper starts with the analysis of the linear response in free and continues to interacting electron-hole plasma focusing on the locality, derived in Eq. (4). Further, we point out two immediate experimental consequences: dependence of the conductance in finite samples on the location of the source, drain, and probes and a peculiar polarization dependence of the light reflection (transmission) off a graphene flake.

II. NONINTERACTING VERSUS INTERACTING NEUTRAL ELECTRON-HOLE PLASMA IN GRAPHENE

Due to its atomic structure, the tight-binding model is a valid starting point in the description of graphene. At energies well below 1 eV, one typically replaces it by an effective Dirac (Weyl) model "near" its two Dirac points constituting the Fermi "surface" of undoped graphene. Neglecting the electron-electron interactions, the linear density-density and current-current response is still local [6,7]:

$$\begin{aligned}\chi(\omega,k) &= \frac{\sigma_0 k^2}{\sqrt{v^2k^2-\omega^2}} = \frac{k^2}{i\omega}\sigma_0 + O(k^4),\\ \sigma_{ij}(\omega,k) &= \frac{i\sigma_0}{\omega\sqrt{v^2k^2-\omega^2}}[\delta_{ij}(\omega^2-v^2k^2)+v^2k_ik_j]\\ &= \sigma_0\delta_{ij} + O(k^2),\end{aligned} \tag{5}$$

where $\sigma_0 = e^2/4\hbar$ is the noninteracting value of conductivity, which is independent of frequency and manifestly local:

$$\sigma_T(\omega,k) = \sigma_L(\omega,k) = \sigma_0 + O(k^2). \tag{6}$$

Of course, due to charge conservation, the transverse conductivity is proportional to the susceptibility [1]:

$$\sigma_T(\omega,k) = \frac{i\omega}{k^2}\chi(\omega,k). \tag{7}$$

The locality is a bit fortuitous since it follows not just from the charge conservation, but in addition, utilizes the pseudorelativistic invariance as well. In a relativistic system, the charge and the current correlators are parts of the polarization tensor $\Pi^{\nu}_{\mu}(k) = \langle J_\mu(k)J^\nu(-k)\rangle$. Here, $J_\mu = \{v\rho,\mathbf{J}\}$ is the $2+1$ current vector. Pseudo-Lorentz transformations relate the current-current part to the density-density components of the tensor. Indeed, the Lorentz invariance together with charge conservation ensures transversality,

$$\Pi_{\mu\nu}(k) = \left(g_{\mu\nu} - \frac{k_\mu k_\nu}{k^\rho k_\rho}\right)A(k), \tag{8}$$

with $g_{00} = 1, g_{ij} = -\delta_{ij}$. The Kubo formula then gives

$$\sigma_{ij}(k) = -\frac{1}{i\omega}\left(\delta_{ij} + \frac{v^2k_ik_j}{\omega^2 - v^2\mathbf{k}^2}\right)A(k), \tag{9}$$

and consequently comparing with Eq. (3),

$$\sigma_T = -\frac{A}{i\omega}; \quad \sigma_L = -\frac{A}{i\omega}\frac{\omega^2}{\omega^2 - v^2\mathbf{k}^2}. \tag{10}$$

In noninteracting graphene $A = \sigma_0\omega^2/\sqrt{v^2\mathbf{k}^2-\omega^2}$ and Eqs. (5) and (6) follow.

Coulomb interactions break the pseudorelativistic invariance, so one has to calculate σ_T (or equivalently the density-density response) and σ_L separately. Assuming a small coupling, the natural approach is to calculate the leading effect of interactions perturbatively [8–12] in α and then supplement it by certain resummations like the random phase resummation (RPA) [7].

To the leading order in α, the results are still frequency independent (see current-current correlator diagrams in Fig. 1),

$$\sigma_1^T(\omega,k) = C_2\sigma_0\alpha + O(k^2), \tag{11}$$

$$\sigma_1^L(\omega,k) = (2C_1 - C_2)\sigma_0\alpha + O(k^2), \tag{12}$$

where $C_1 = 25/12 - \pi/2 \approx 0.51$ and $C_2 = 19/12 - \pi/2 \approx 0.01 \ll 1$. The constants C_1 and C_2 were actually obtained in the continuum Dirac theory some time ago and were a subject of a long controversy. This note is devoted also to a further clarification of this point. The general belief apparently was that there should be a single value of the coefficient C determining the whole conductivity tensor due to locality, $\sigma_{xx} = \sigma_{yy} = \sigma_L = \sigma_T$. The current-current correlator $\langle J_xJ_x\rangle$ calculation utilizing a sharp momentum cutoff Λ regularization of the Dirac model by Herbut, Juričić, and Vafek [8] can be interpreted as Eq. (12) using a local combination (trace) $\sigma^1_{xx} + \sigma^1_{yy} = \sigma_1^T + \sigma_1^L = 2C_1\sigma_0\alpha$. It is important to calculate this combination, since σ_{xx} is ill defined in the $k_x, k_y \to 0$ limit according to Eq. (3). We have recalculated this

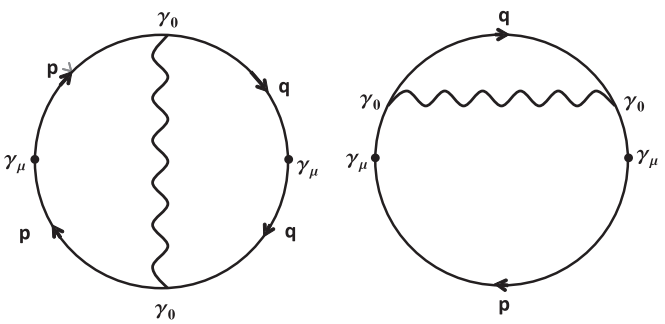

FIG. 1. Leading order diagrams for the interaction corrections to both the current-current ($\mu = 1,2$) and density-density ($\mu = 0$) correlators. Left: the vertex part; right: the self-energy part.

calculation using the tight-binding model [13] with the same result, see Ref. [14]. The use of the sharp momentum cutoff was criticized by Mishchenko [9], who employed a "soft" momentum cutoff regularization, a Λ dependent modification to the Coulomb potential. In addition to the current-current correlator, he calculated the density-density correlator which, using charge conservation (7), leads to Eq. (11). He supported this choice of regulator by demanding the aforementioned "consistency" between the $\langle\rho\rho\rangle$ and the $\langle JJ\rangle$ calculation via a local version of charge conservation, $k^2\sigma_{xx} = i\omega\chi$, instead of the exact one, $k_i\sigma_{ij}k_j = i\omega\chi$, which is valid for nonlocal electrodynamics as well (and in addition to the kinetic equation approach). We have performed the tight-binding calculation of $\langle\rho\rho\rangle$ and found the same value (that was also obtained by other groups in continuum [11,12]), but the $\langle JJ\rangle$ calculation is inconsistent with the tight-binding result, see Ref. [14] for details. Thus the two different values of C *do not contradict each other*, but rather demonstrate nonlocality of the graphene electrodynamics.

The tight-binding calculations are quite tedious and therefore one would like to formulate a consistent cutoff procedure within the continuum Dirac model. An attempt to formulate such a condition for a regularization of the continuum model consistent with the tight-binding model is done in Ref. [15], where several calculations inconsistent with it are analyzed. Having established Eqs. (3), (11), and (12), let us turn to the observable effects of the unconventional nonlocal component of the conductivity in electric transport and optics.

III. EFFECTS OF NONLOCAL ELECTRODYNAMICS IN TRANSPORT

The nonlocal term in the conductivity of graphene renders the electrodynamics rather unusual. Transport experiments on cleanest samples (ac conductivity in optical and near infrared range [16,17] in graphene on substrates and dc conductivity measurements in suspended graphene and on NiB_2 substrates [4]) indicate that the deviations from the noninteracting conductivity value σ_0 is very small. It has been pointed out by Sheehy and Schmalian [18] that the "accidentally" small value $C_2 = 0.01$ is consistent with the experiments, while $C_1 = 0.51$ is not. Consider stationary situations.

Generally, a vector field decomposes (for a simply connected flake) into an irrotational and a solenoidal vector field, so that the two-dimensional current density can be expressed in terms of two scalar fields u and h,

$$J_i(r) = J_i^{\text{irrot}} + J_i^{\text{sol}} = \partial_i u(r) + \varepsilon_{ij}\partial_j h(r), \tag{13}$$

where ε_{ij} is the two-dimensional Levi-Civita symbol. The electric field created by the current is $E_i = \rho_{ij}J_j$, with the resistivity tensor obtained by inversion of Eq. (3),

$$\rho_{ij}(\omega,\mathbf{k}) = \rho_T\delta_{ij} + \rho_{\text{nl}}\frac{k_i k_j}{k^2}, \tag{14}$$

with $\rho_T = \sigma_T^{-1}$ and $\rho_{\text{nl}} = \sigma_{\text{nl}}/\sigma_T(\sigma_T - \sigma_{\text{nl}}) \simeq \frac{\alpha}{\sigma_0}$. In terms of the "potentials" of Eq. (13) the electric field is written as

$$E_i = \rho_T J_i + \rho_{\text{nl}}\partial_i u, \tag{15}$$

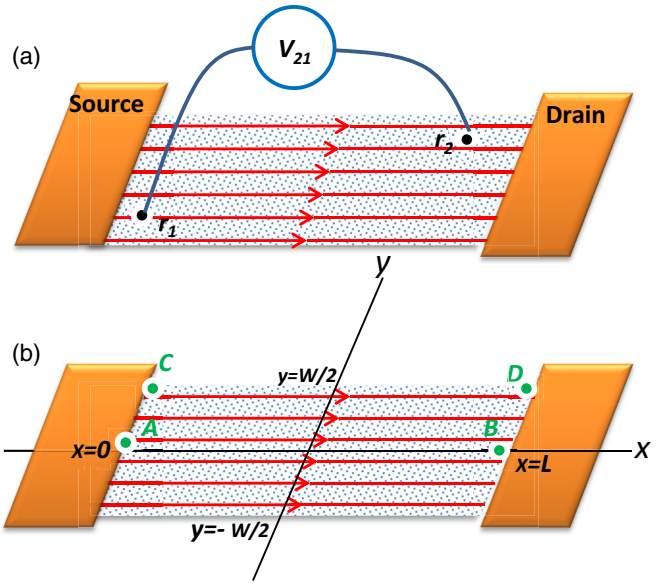

FIG. 2. (Color online) (a) A typical transport measurement in graphene. The current enters and leaves via the leads, while the voltage is measured between different points. (b) The location of the voltage probes: $A = 0,0$, $B = L,0$ for the source - to - drain direction x; $C = 0,W/2$ and $D = L,W/2$ for the "off diagonal" direction y.

where the first term is the local, regular (pseudo) Ohmic and the second term is the nonlocal contribution. The line integral over the electric field inside the graphene flake $V = -\int \mathbf{E}\cdot d\mathbf{l}$ (that does not depend on the contour in our case) is

$$V(\mathbf{r}_1,\mathbf{r}_2) = V_{\text{loc}} + \rho_{\text{nl}}[u(\mathbf{r}_2) - u(\mathbf{r}_1)]. \tag{16}$$

The first term coincides with the voltage of a metallic flake with resistivity ρ_T.

From the definition in Eq. (13) and from the (stationary) charge conservation, it follows that $u(\mathbf{r})$ obeys the Poisson equation

$$\nabla^2 u(\mathbf{r}) = \partial_i J_i(\mathbf{r}) = -\partial_z J_z(\mathbf{r},z)|_{z=0} \equiv s(\mathbf{r}). \tag{17}$$

More generally, the last term in Eq. (17) refers to the current entering and leaving via the leads, see Fig. 2(a) . The source or drain are either pointlike, linelike near the surface, or cover an area like in suspended samples experiments. The solution to Eq. (17) is

$$u(\mathbf{r}) = -\frac{1}{2\pi}\int_{\mathbf{r}'\in\text{flake}} \ln|\mathbf{r}-\mathbf{r}'|s(\mathbf{r}'), \tag{18}$$

and various shape dependencies are studied in Ref. [19].

Let us consider a simple example of application of that nonlocal electrodynamics to a transport experiment with boundary conditions leading to the homogeneous current density shown in Fig. 2(a). For a rectangular flake with a linelike source and drain (golden bars in Fig. 2), the resistance between the points $A = \{0,0\}$ and $B = \{L,0\}$ has a nonlocal correction:

$$R_{\text{nl}}^{BA} = \rho_{\text{nl}}\left[\frac{2}{\pi\chi}\arctan\left(\frac{\chi}{2}\right) + \frac{1}{2\pi}\ln(4\chi^{-2}+1)\right], \tag{19}$$

where $\chi = W/L$ is the aspect ratio of a flake of length L and width W . The shape-dependent factor vanishes as $1/\chi$ for

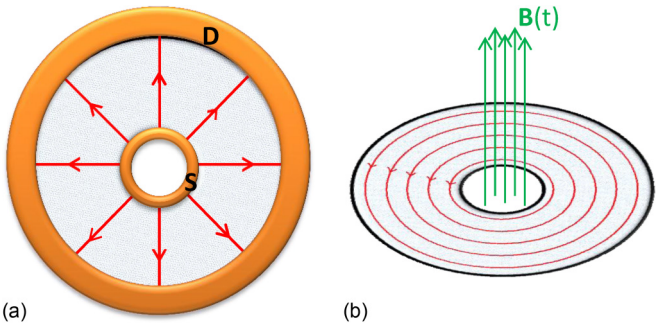

FIG. 3. (Color online) A graphene Corbino disk. (a) A radial current enters and leaves via the leads. (b) The circular current generated by a magnetic flux increasing linearly in time.

$L \ll W$ and is still sublinear, $-\frac{1}{\pi}\ln(\chi)$, when $L >> W$. For typical aspect ratio of $\chi = 1$ (square), it is 0.55. This differs from the nonlocal contribution when the probes are attached at corners $C = \{0, W/2\}$ and $D = \{L, W/2\}$,

$$R_{\rm nl}^{\rm DC} = \rho_{\rm nl}\left[\frac{1}{\pi\chi}\arctan(\chi) + \frac{1}{4\pi}(\chi^{-2}+1)\right], \qquad (20)$$

which for the square sample is smaller, 0.31. The local contribution is independent of the location along the leads. This property can be used to isolate the nonlocal contribution. The conductivity σ_{xx} deduced from such measurement depends therefore on the aspect ratio and even on the location of the probes. The interaction corrections might not be that negligible as it would follow from the unnaturally small correction to σ_0 in the local part $\sigma_T = \sigma_0\alpha C_2 = 0.01\sigma_0\alpha$. The nonlinearity allows a direct determination of the interaction strength α. Moreover, there is a voltage in the direction perpendicular to current. Although the voltage drop from side to side vanishes due to the reflection symmetry, the voltage between points A and C near a lead is maximal:

$$R_{\rm Hall}^{CA} = \rho_{\rm nl}\left\{\frac{1}{\pi\chi}\left[\arctan(\chi) - 2\arctan\left(\frac{\chi}{2}\right)\right] + \frac{1}{2\pi}\ln\left(\frac{\chi^2+1}{\chi^2+4}\right)\right\}, \qquad (21)$$

for the square it gives $R_{\rm Hall}^{CA} = -0.19\rho_{\rm nl}$.

A clear manifestation of the effect of geometry of leads on resistance can be provided by a graphene Corbino disk with internal and external radii r_1 and r_2, see Fig. 3 . While the radial current, Fig. 3(a), leads to a nonlocal resistance of $R_{\rm nl} = \frac{\rho_{\rm nl}}{2\pi}\ln\frac{r_2}{r_1}$, the circular current, Fig. 3(b) (generated by a magnetic flux increasing linearly in time threading the disk) has no source and hence the correction vanishes.

The nonlocality becomes apparent in the optical response of a graphene flake [20]. The reflectivities of the p and s polarizations of electromagnetic waves scattered at angle θ, see Fig. 4 , are

$$r_p(\omega) = -\frac{\pi\cos\theta}{c}(\sigma_T + \sigma_{\rm nl}),$$
$$r_s(\omega) = -\frac{\pi\sigma_T}{c\cos\theta + \pi\sigma_T}. \qquad (22)$$

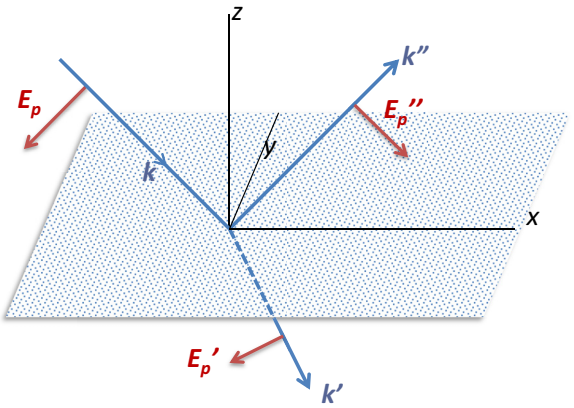

FIG. 4. (Color online) A typical optical reflection experiment. For the shown p polarization the electric field lies in the plane of incidence.

The derivations and assumptions are given in Ref. [21]. Note that the reflectivities (and transmissivities) are independent of frequencies below the visible range. Although the expressions are given for zero temperature, the dependence on temperature is not expected to be strong, unless phonons have an effect at lower frequencies. The polarization dependence appears despite the time reversal invariance (no magnetic field here, unlike in the Faraday effect in graphene [22]), and absence of anisotropy. There is no dramatic change in the equations for the surface waves or plasmons [23], at least at zero temperature.

IV. CONCLUSIONS, DISCUSSIONS, AND POSSIBLE GENERALIZATIONS

The calculation of the leading Coulomb interaction effect on the electromagnetic response of undoped graphene reveals that its macroscopic electrodynamics becomes nonlocal in a sense that the wave-vector-dependent ac conductivity tensor becomes nonanalytic at small wave vectors, see Eq. (3). The origin of nonlocality is a combination of the long-range (unscreened) Coulomb interactions and the ultrarelativistic nature of the quasiparticles. Several distinct experimental signatures of the nonlocal contribution to conductivity, Eq. (4), were pointed out. The resistance of the graphene flake depends on the location and the geometry of source, drain, and probes. In some configurations like a circular Corbino geometry, Fig. 3(b), void of sources or drains, the nonlocal voltages are absent, while in others, like the radial current flow of Fig. 3(a), they are maximized. In rectangular samples typically used in transport experiments, a quite strong geometrical factor complicates the analysis of the relation between resistance and the *two* resistivities, ρ_T and $\rho_{\rm nl}$, Eq. (14). Voltages perpendicular to the current appear close to the source or the drain in this time-reversal symmetric situation. The relation between the dielectric constant and conductivity, Eq. (7), is distinct from either a metal or an insulator. Nonlocality causes a polarization modification of the reflected and transmitted light proportional to the Coulomb interaction strength α, without either the magnetic field, like in the Faraday effect, or anisotropy in the optically active materials.

The treatment is perturbative so let us discuss whether the available graphene samples have sufficiently small coupling for it to be reliable. A recent, rather confident measurement [24] of the coupling in graphene on a h-BN substrate (from velocity renormalization and scattering off impurities at a controllable small chemical potential) gives $\alpha = 0.78$. We argue that this value is small enough to use perturbation theory. The argument is a variant of the "Georgi's loop factor in quantum electrodynamics." The real dimensionless expansion parameter in perturbation theory is not α, but rather $\alpha' = a/G$, where G is the geometrical factor, $G^2 = \frac{A_D}{2(2\pi)^{D+1}}$, where A_D is the surface area of D-dimensional unit sphere. In our case of $D = 2$, $G = 2\pi$, so that, at least, for $\alpha = 0.78$, $\alpha' = 0.12 \ll 1$. Note that there is a rather large dielectric constant of the substrate $\varepsilon_{\rm BN} = 3$–4; at this point, it is not clear what is the coupling in suspended samples (the corrections to the conductivity are small, no chiral condensate is observed, and there is no substrate dielectric constant). There has been an ongoing debate concerning the strength of the interelectron interactions in undoped graphene. Although naively the coupling α can be of order one in suspended samples [7], there is evidence that the actual coupling is in fact weak. If it were strong (of order 1), it would lead to the chiral condensate [25], making the excitations gapped. This was shown nonperturbatively by the lattice (tight-binding) simulation [26] and recently reconfirmed by Refs. [27–29]. Experiments observe a rather strong renormalization of the Fermi velocity, but no condensation [30].

There are several phenomena that might mask the nonlocal electrodynamics effects. One could be disorder, another is a nonzero chemical potential. One should distinguish the case of homogeneous doping from puddles that appear naturally in samples on substrates. If the homogeneous chemical potential μ is so small that the screening length, $v_g^2\hbar^2/e^2\mu$, is of the order of the sample size L, it can be ignored. For a typical length of $L = 0.1$ to $1\ \mu$m and absolutely clean samples (disorder reduces screening) this translates to $\mu = 3\,$meV $=$ 35 K and $0.3\,$meV $= 3.5$ K, respectively. If the screening is significant, our resistivity formulas should be applied only within the skin depth of the flake. An important issue here is to separate contributions between two channels, the interband (which is the one considered in the present calculation and generally quite insensitive to disorder [31], and the intraband channel when one has quite an ordinary generally diffusive motion of electrons in the conduction band. As mentioned in Introduction, the diffusive motion of the "additional" electrons obeys $\sigma_T = \sigma_L$, and thus does not contribute to the nonlocal effects. It makes, however, the detection of these effects more complicated since one needs to either subtract them or reliably calculate them. The two channels are not completely separated due to the Pauli blocking, this is, however, expected to be insignificant for small chemical potential.

If the sample is not suspended (in suspended samples charge "puddles" were not seen), one typically has a small chemical potential due to the substrate, etc., even if the gate voltage is tuned to the Dirac point. Suppose the puddles have extent l and chemical potential of order μ (of both signs). Then screening can be definitely neglected when $l < v_g^2\hbar^2/(e^2\mu)$ and even for larger l the disorder (puddles id the disorder) makes screening less effective. How small can the screening length be? In Ref. [32], graphene on a SiO_2 substrate was modeled. The case of the carrier density in a puddle of $n = 2.5 \times 10^{11}\ {\rm cm}^{-1}$ corresponds to $\mu = 13\,$meV $= 150\,$K and the screening length 20 nm is of the order of the puddle $l = 5$ nm. So we do not expect that puddles in good samples will interfere with nonlocal conductivity effects. Recently, NB substrates are widely used and the problem is greatly reduced there, see, for example, Ref. [33].

The 2D Dirac electrons appear also in other condensed matter systems, for example, on the surface of a topological insulator [34]. Note, however, that in order to prevent screening on the scale of the sample size, the chemical potential should be tuned precisely to the Dirac point and the sample should be very clean. Nonlocal 3D conductivity is expected to occur also in recently discovered 3D Dirac point materials like in Ref. [5]. Electron-electron interactions have been already studied there theoretically [35,36].

ACKNOWLEDGMENTS

We are indebted to W.B. Jian, I. Herbut, E. Farber, C. W. Luo, S. Sternklar, D. Cheskis, H. Fertig for valuable discussions, and M. Fogler for correspondence. Work of B.R. and H.K. was supported by NSC of R.O.C. Grant Nos. 98-2112-M-009-014-MY3 and 101-2112-M-003-002-MY3, respectively, and MOE ATU program.

[1] G. Giuliani and G. Vignale, *Quantum Theory of the Electron Liquid* (Cambridge University Press, Cambridge, 2005).
[2] A. H. Castro Neto, F. Guinea, N. M. R. Peres, K. S. Novoselov, and A. K. Geim, Rev. Mod. Phys. **81**, 109 (2009).
[3] X. Du, I. Skachko, A. Barker, and E. Y. Andrei, Nat. Nanotechnol. **3**, 491 (2008).
[4] A. S. Mayorov, D. C. Elias, I. S. Mukhin, S. V. Morozov, L. A. Ponomarenko, K. S. Novoselov, A. K. Geim, and R. V. Gorbachev, Nano Lett. **12**, 4629 (2012).
[5] M. Orlita, D. M. Basko, M. S. Zholudev, F. Teppe, W. Knap, V. I. Gavrilenko, N. N. Mikhailov, S. A. Dvoretskii, P. Neugebauer, C. Faugeras, A. L. Barra, G. Martinez, and M. Potemski, Nat. Phys. **10**, 233 (2014).
[6] A. Principi, M. Polini, and G. Vignale, Phys. Rev. B **80**, 075418 (2009).
[7] V. N. Kotov, B. Uchoa, V. M. Pereira, F. Guinea, and A. H. Castro Neto, Rev. Mod. Phys. **84**, 1067 (2012).
[8] I. F. Herbut, V. Juričič, and O. Vafek, Phys. Rev. Lett. **100**, 046403 (2008).
[9] E. G. Mishchenko, Europhys. Lett. **83**, 17005 (2008).
[10] V. Juričič, O. Vafek, and I. F. Herbut, Phys. Rev. B **82**, 235402 (2010).
[11] S. H. Abedinpour, G. Vignale, A. Principi, M. Polini, W. K. Tse, and A. H. MacDonald, Phys. Rev. B **84**, 045429 (2011).
[12] I. Sodemann and M. M. Fogler, Phys. Rev. B **86**, 115408 (2012).

[13] B. Rosenstein, M. Lewkowicz, and T. Maniv, Phys. Rev. Lett. **110**, 066602 (2013).
[14] See Supplemental Material at http://link.aps.org/supplemental/10.1103/PhysRevB.90.045137 for the tight binding calculation of the interaction corrections to conductivity.
[15] See Supplemental Material at http://link.aps.org/supplemental/10.1103/PhysRevB.90.045137 for the cutoff procedure in continuum Dirac model consistent with the tight binding model.
[16] R. R. Nair, P. Blake, A. N. Grigorenko, K. S. Novoselov, T. J. Booth, T. Stauber, N. M. R. Peres, and A. K. Geim, Science **320**, 1308 (2008).
[17] K. F. Mak, M. Y. Sfeir, Y. Wu, C. H. Lui, J. A. Misewich, and T. F. Heinz, Phys. Rev. Lett. **101**, 196405 (2008).
[18] D. E. Sheehy and J. Schmalian, Phys. Rev. B **80**, 193411 (2009).
[19] See Supplemental Material at http://link.aps.org/supplemental/10.1103/PhysRevB.90.045137 for effects of nonlocal electrodynamics in transport in various geometries.
[20] L. A. Falkovsky and S. S. Pershoguba, Phys. Rev. B **76**, 153410 (2007).
[21] See Supplemental Material at http://link.aps.org/supplemental/10.1103/PhysRevB.90.045137 for effects of nonlocal electrodynamics in optics.
[22] I. Crassee, J. Levallois, A. L. Walter, M. Ostler, A. Bostwick, E. Rotenberg, T. Seyller, D. van der Marel, and A. B. Kuzmenko, Nat. Phys. **7**, 48 (2011).
[23] S. Das Sarma and Q. Li, Phys. Rev. B **87**, 235418 (2013).
[24] D. A. Siegel, W. Regan, A. V. Fedorov, A. Zettl, and A. Lanzara, Phys. Rev. Lett. **110**, 146802 (2013).
[25] D. V. Khveshchenko, Phys. Rev. Lett. **87**, 246802 (2001).
[26] J. E. Drut and T. A. Lähde, Phys. Rev. Lett. **102**, 026802 (2009).
[27] W. Armour, S. Hands, and C. Strouthos, Phys. Rev. B **84**, 075123 (2011).
[28] P. V. Buividovich, E. V. Luschevskaya, O. V. Pavlovsky, M. I. Polikarpov, and M. V. Ulybyshev, Phys. Rev. B **86**, 045107 (2012).
[29] M. V. Ulybyshev, P. V. Buividovich, M. I. Katsnelson, and M. I. Polikarpov, Phys. Rev. Lett. **111**, 056801 (2013).
[30] D. C. Elias, R. V. Gorbachev, A. S. Mayorov, S. V. Morozov, A. A. Zhukov, P. Blake, L. A. Ponomarenko, I. V. Grigorieva, K. S. Novoselov, F. Guinea, and A. K. Geim, Nat. Phys. **7**, 701 (2011).
[31] M. Lewkowicz, B. Rosenstein, and D. Nghiem, Phys. Rev. B **84**, 115419 (2011).
[32] M. Gibertini, A. Tomadin, F. Guinea, M. I. Katsnelson, and M. Polini, Phys. Rev. B **85**, 201405(R) (2012).
[33] F. Amet, J. R. Williams, K. Watanabe, T. Taniguchi, and D. Goldhaber-Gordon, Phys. Rev. Lett. **110**, 216601 (2013).
[34] B. Yan and S. C. Zhang, Rep. Prog. Phys. **75**, 096501 (2012).
[35] P. Hosur, S. A. Parameswaran and A. Vishwanath, Phys. Rev. Lett. **108**, 046602 (2012).
[36] B. Rosenstein, and M. Lewkowicz, Phys. Rev. B **88**, 045108 (2013).